Shale gas potential of the Mowry Shale in Wyoming Laramide basins

Wyoming State Geological Survey
Challenges in Geologic Resource Development No. 9

Ronald C. Surdam, Zunsheng Jiao, Rodney H. De Bruin, and Ramsey D. Bentley

Wyoming State Geological Survey
Ronald C. Surdam, State Geologist

First printing of 500 copies by Citizen Printing, Fort Collins, Colorado, September 2010.

Shale gas potential of the Mowry Shale in Wyoming Laramide Basins, by Ronald C. Surdam, Zunsheng Jiao, Rodney H. DeBruin, and Ramsey D. Bentley.
Wyoming State Geological Survey Challenges in Geologic Resource Development No. 9, 2010.
ISBN 1-884589-55-3

Cover photos: Outcrop of Mowry Shale near Casper, Wyoming, under a summer thunderstorm. *Photos by Meg Ewald.*

Shale gas potential of the Mowry Shale in Wyoming Laramide basins

Wyoming State Geological Survey
Challenges in Geologic Resource Development No. 9

Ronald C. Surdam, Zunsheng Jiao, Rodney H. De Bruin, and Ramsey D. Bentley

TABLE OF CONTENTS

Figures

Tables

Abstract

The Cretaceous Mowry Shale in Wyoming is an outstanding source rock and a potential shale-gas target. Total organic carbon (TOC) content of the Mowry Shale ranges from 0.7 percent to 5.1 percent. In Wyoming, the thickness of the Mowry Shale decreases from approximately 600 feet in the northwest part of the state to approximately 250 feet in the southeast part, whereas the TOC content of the Mowry increases from northwest to southeast. T_{max} for Mowry samples ranges from 411° C to 455° C. Vitrinite reflectance values range up to 1.7 at present-day depths greater than 10,000 feet. Displacement pressures range from 300 pounds per square inch (psi) at 500 feet present-day burial depth to more than 2,000 psi at 13,000 feet. The ^{13}C nuclear resonance spectra indicate that the aliphatic carbon peak of the Mowry Shale is greatly diminished at 13,000 feet. Therefore, the kerogen remaining in the formation at this depth has very little capacity to generate liquid or gaseous hydrocarbons. Thermal maturation modeling suggests that for each gram of TOC in the Mowry Shale, about 80 milligrams (mg) of gas was generated, 18 mg of gas was expelled, and 62 mg of gas remains stored in the shale. Sonic and seismic interval velocities show a pronounced slowdown where significant quantities of natural gas remain in the Mowry Shale. The attributes of the Mowry Shale described above suggest that it has significant potential as a shale-gas prospect. With new drilling and completion techniques, the recovery of natural gas remaining in the Mowry could be substantial.

Introduction

This paper explores the shale-gas potential of the Wyoming Cretaceous shale section in general, and of the Mowry Shale in particular. The Mowry Shale serves as a good shale-gas surrogate for the lower Cretaceous shale sequence in Wyoming. Most importantly, as a stratigraphic unit, it is easily recognized in outcrop (**Figure 1**) and in the subsurface (i.e., geophysical log signature; **Figure 2**). The Mowry Shale, along with the other organic-rich portions of the Cretaceous stratigraphic section, has long been recognized as a prolific hydrocarbon source rock in the Rocky Mountain Laramide basins. Another characteristic of the Mowry Shale important to the evaluation of shale-gas plays in Wyoming is the consistent mineralogy and lithology of the unit. Statewide mineralogical and lithological variations of the Mowry Shale will be discussed later in the paper.

The Mowry Shale

The Mowry Shale was deposited in an inland sea that covered all of Wyoming during the transition from lower to upper Cretaceous (Byers and Larson, 1979). Although the Mowry Shale consists of several lithofacies, the rock unit is best known for the organic-rich siliceous shale facies (**Figure 1**). The siliceous shale facies is by far the most abundant rock type in the Mowry and occurs almost everywhere the unit occurs. Other relatively minor lithofacies in the Mowry are nonsiliceous silty shale, sandstone, and cristobalitic shale (Davis, 1970). In Wyoming, these minor lithofacies typically become abundant in the southeast and northwest portions of the Mowry depositional system (Davis, 1970).

The Mowry Sea and stratigraphic relations

During the transition from lower to upper Cretaceous, the Western Interior Foreland Basin of North America was flooded and drained by successive marine transgressions and regressions (Davis et al., 1989). During maximum marine transgressions, the inland sea was continuous from the Arctic Ocean to the Gulf of Mexico (Kauffman, 1977). In contrast, during maximum marine regressions, the seaway was nearly drained and was cut off from the Gulf of Mexico (**Figure 3**). During the transition from lower to upper Cretaceous, the Mowry inland sea (**Figure 4**) transgressed over a variety of depositional environments; in Wyoming, it transgressed over a predominantly marine/fluvial depositional environment (i.e., Muddy Sandstone). This marine/fluvial depositional system produced the Muddy sandstone (Dolson et al., 1991), a complex unit consisting mainly of shoreface and valley-filled sandstones and a variety of finer-grained facies. The Muddy Sandstone in Wyoming is recognized as a significant oil and gas reservoir that overlies organic-rich shales (i.e., Skull Creek Shale) and underlies the organic-rich Mowry Shale (**Figure 4**).

The Mowry Shale was deposited over a period of several million years (Obradovich and Cobban, 1975; Williams and Stelek, 1975) in the southern portion of the inland seaway (**Figure 3**). The Mowry sea has been described as an oxygen-poor stratified basin (Davis, 1970; Byers

Figure 1. Mowry Shale outcrop along State Highway 220, south of Casper, Wyoming. The organic-rich siliceous shale is the dominant lithofacies in the Mowry shale. Other minor lithofacies in the Mowry Shale are nonsiliceous silty shale, a thin sandstone layer, and cristobalitic shale.

Figure 2. Typical well log of the Mowry Shale characterized by high gamma ray counts, lower interval velocities, and higher resistivities.

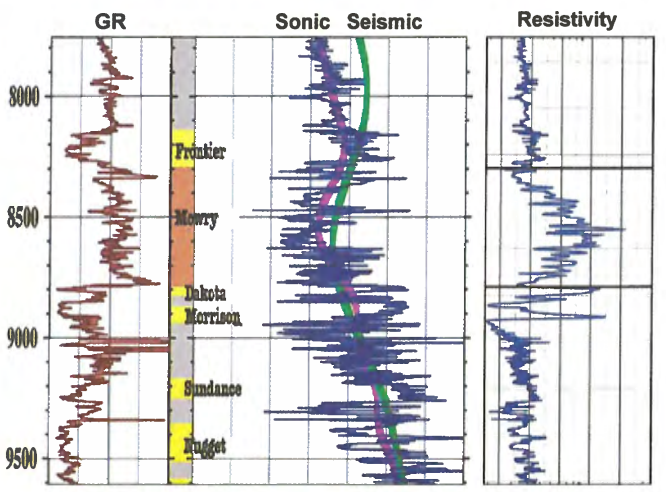

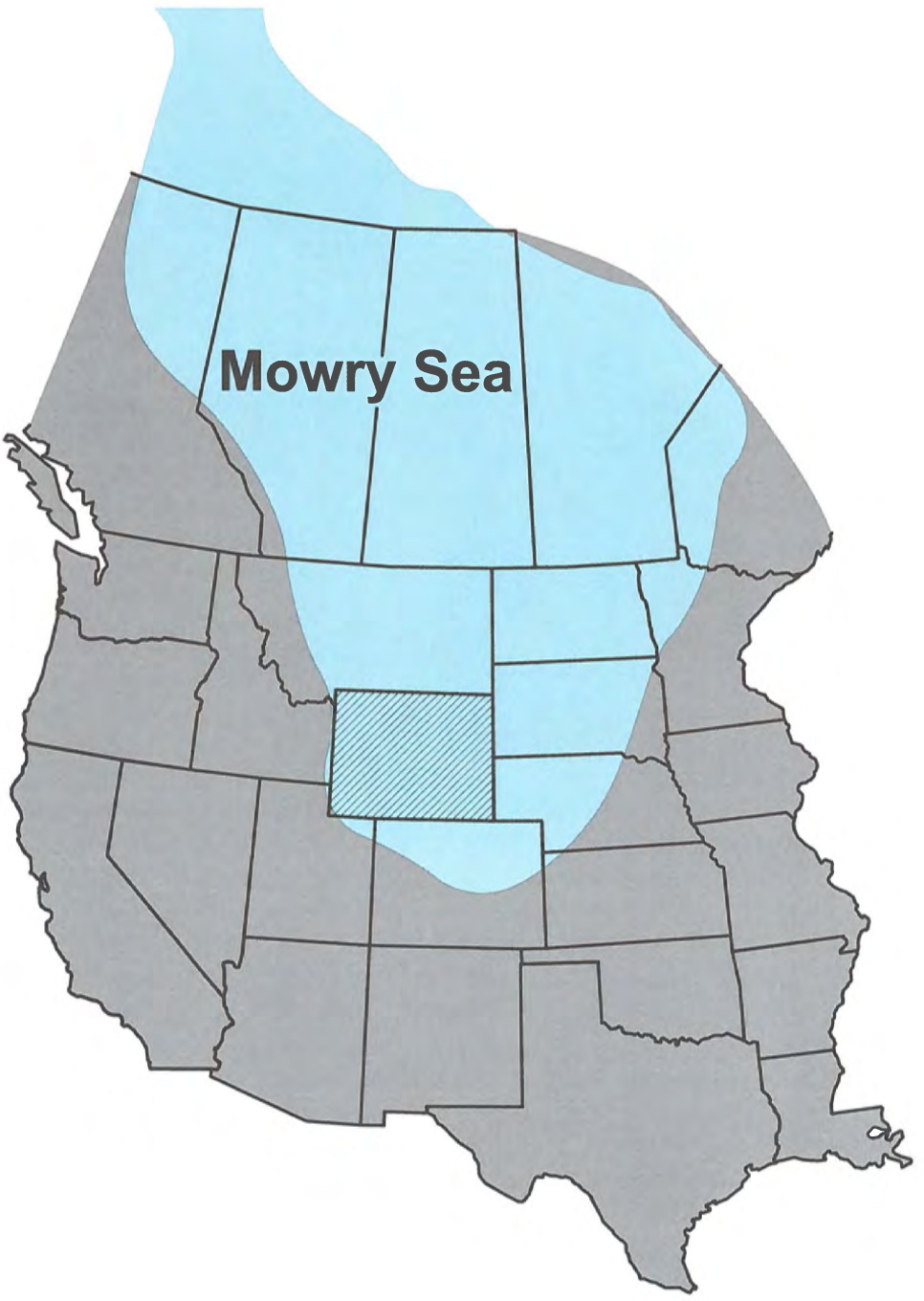

Figure 3. The Mowry Sea during the transition from lower to upper Cretaceous is shown in green on the map. During this time, the Western Interior Foreland Basin in the Rocky Mountain region was flooded and drained by successive marine transgressions and regressions. *Modified from Davis et al., 1989.*

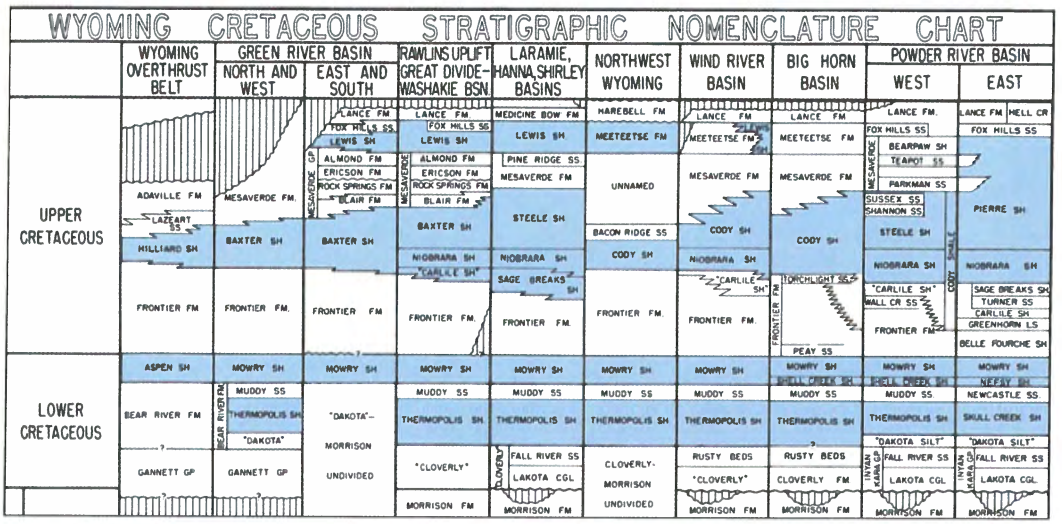

Figure 4. Wyoming Cretaceous stratigraphic nomenclature chart. The Mowry Sea transgressed over a variety of depositional systems: in Wyoming, it transgressed over a predominantly marine/fluvial depositional system (Muddy Sandstone). *Modified from the Wyoming Geological Association 44th Annual Field Conference Guidebook.*

and Larson, 1979). As a result, the Mowry Shale is typically a widespread, fine-grained, organic-carbon-rich shale.

Regional Mowry Shale stratigraphic relations and nomenclature in Wyoming Laramide basins (WLB) are illustrated in **Figure 4**. The distribution of the Mowry Shale, including stratigraphically equivalent units such as the Aspen Shale, is shown in **Figure 4**. The Mowry Shale crops out at the margins of all WLB (**Figure 5**).

In most WLB, the Mowry Shale typically underlies the Frontier Formation (or the equivalent Belle Fourche Shale in the Powder River Basin (PRB)). The Frontier Formation is characterized by a complex depositional system composed of alternating shales and marine sandstones.

Mowry Shale characteristics

Total organic carbon (TOC) content of the Mowry Shale in WLB ranges from one to five percent (**Figure 6**). Typically, the average TOC content of the Mowry Shale in the WLB increases from northwest to southeast across Wyoming. This variation in TOC content resulted from the regional dispersal of clastic debris from Cretaceous highlands to the west and northwest of the Mowry Sea during deposition of the Mowry Shale. The Mowry Shale thins from about 600 feet thick in northwestern Wyoming to about 250 feet thick in southeastern Wyoming. Another observation derived from a small sample set is a general decrease in TOC content from shallow to deeper present-day depths of burial (**Figure 6**).

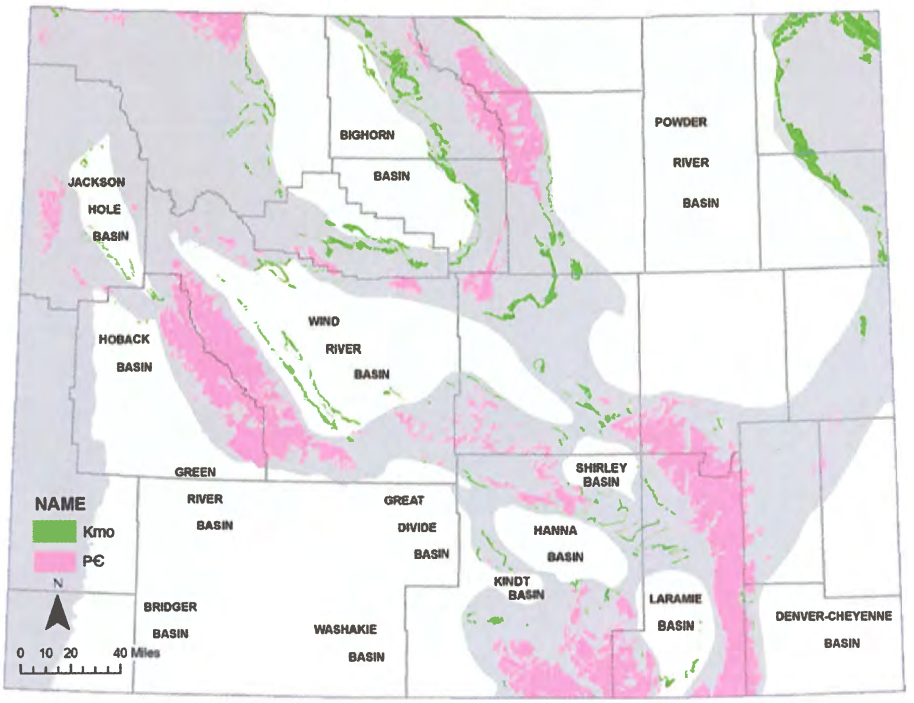

Figure 5. Map showing the outcrop distribution of the Mowry Shale in Wyoming. The Mowry Shale crops out at the margins of all Wyoming Laramide basins.

Clay diagenesis

The diagenesis of mixed-layer illite/smectite (I/S) clays during progressive burial is widely recognized as an important empirical diagenetic geothermometer (Burst, 1969; Hower et al., 1976; Boles and Franks, 1979; Hower, 1981; Pytte and Reynolds, 1989). The diagenetic trend in I/S clay is known to be temperature-dependent and may be related to regional hydrocarbon generation (Bruce, 1984; Hagen and Surdam, 1984). Several authors (Hower, 1981; Pytte and Reynolds, 1989) indicate that the main compositional and structural changes in the I/S burial diagenetic sequence (i.e., increasing thermal exposure) are as follows:

1) An increase in illite layers;
2) An increase in interlayer potassium;
3) An increase in the amount of aluminum substituted for silicon in the tetrahedral layer; and
4) The release of Mg^{2+}, Fe^{2+}, Ca^{2+}, Si^{+}, Na^{2+}, and water. Water released during the smectite → illite reaction can constitute ≤ 35 percent of the volume of the original smectite crystallite (Petty and Hower, 1972).

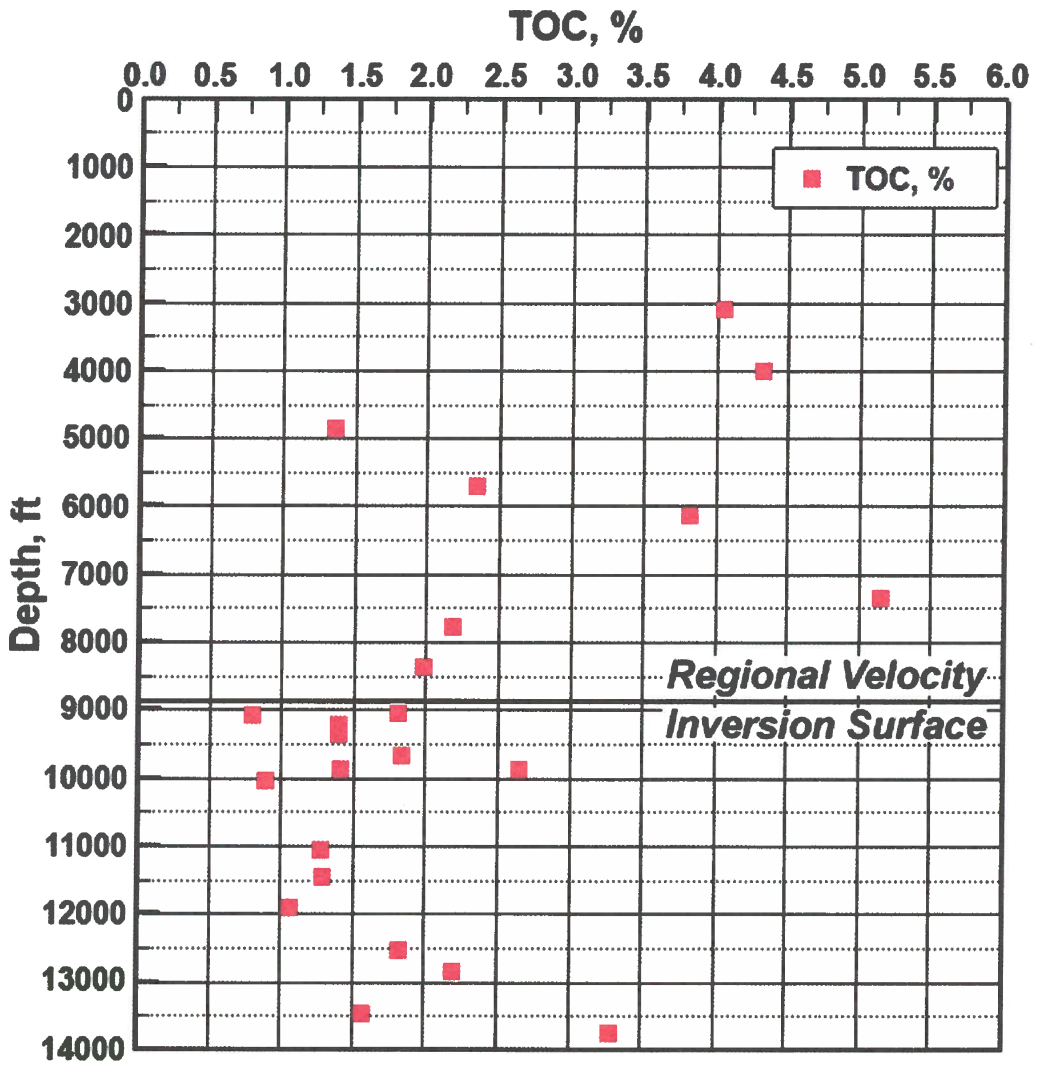

Figure 6. Plot of total organic carbon (TOC) versus depth for Mowry Shale samples from the Powder River Basin, Wyoming. Percentage of TOC generally deceases below the regional velocity inversion surface because of the thermal maturity. *Modified from Jiao, 1992.*

In the WLB, these compositional and structural changes significantly influenced the porosity and permeability of the Cretaceous shales in general, and the development of basin-wide pressure (i.e., fluid flow) compartments (Surdam et al., 2005). The cations released during the smectite → illite transition also affect the porosity and permeability of adjacent sandstones due to the precipitation of quartz, chlorite, kaolinite, and late carbonate cement, further reducing pore space.

As shown by a set of Mowry Shale samples from four WLB (**Figure 7**), the major diagenetic events that occurred in the WLB were the transformation of smectite to illite, the transformation of kaolinite to chlorite, and the ordering of the mixed-layer I/S clays. **Figure 8** shows the x-ray diffraction patterns of the clay-size fraction from the Mowry Shale between 3,600

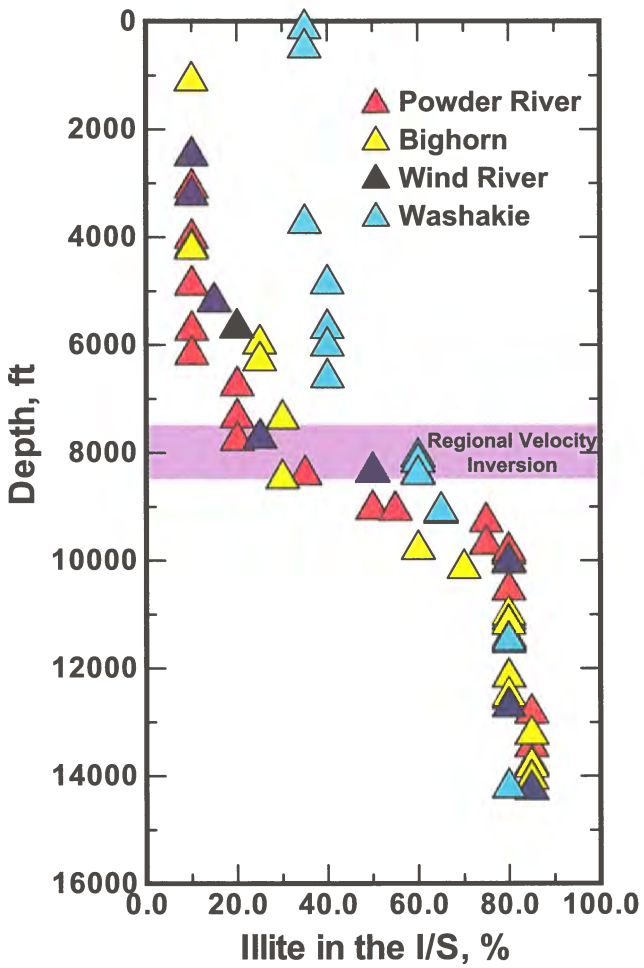

Figure 7. Plot of percent illite in the mixed-layer illite/smectite clays vs. present-day depth for the Cretaceous shales in the Wyoming Laramide basins. *Modified from Jiao and Surdam, 1997.*

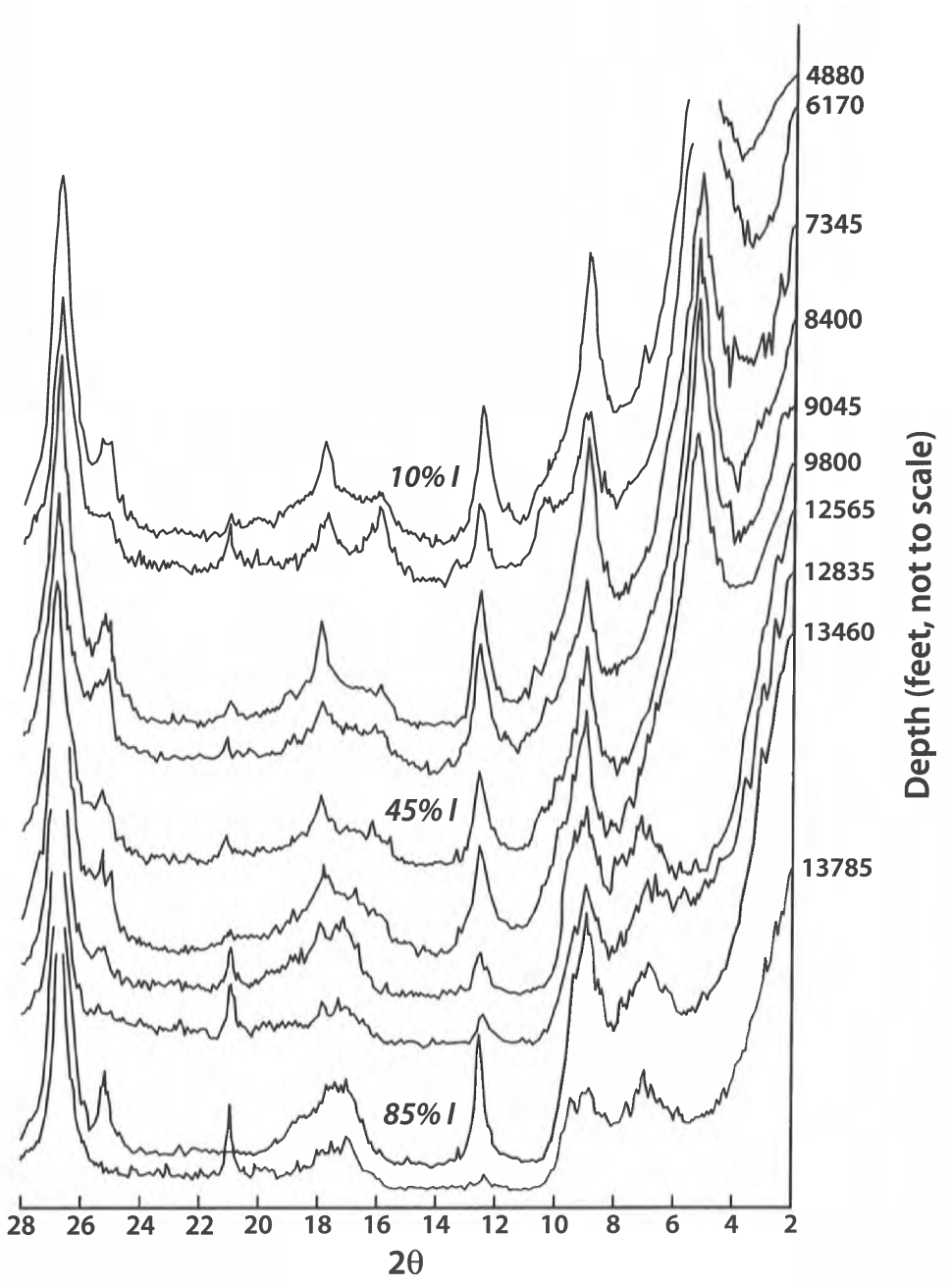

Figure 8. X-ray diffractograms of ethylene-glycolate treated samples (<0.5 μm fraction) of the Mowry Shale in the Powder River Basin, Wyoming. With increasing burial depth, smectite alters to illite in the mixed-layer illite/smectite clays as indicated by the 5.2° 2θpeak shifting to 6.6° 2θ. The structure of the mixed-layer illite/smectite clays changes from random to ordered at approximately 10,000 feet, as indicated by the advent of the 6.6° 2θ peak. The content of chlorite also increases with progressive burial *From Jiao, 1992.*

feet and 14,000 feet at present-day depths in the PRB. **Figure 7** shows the percentage of illite in the mixed-layer I/S clays from the Cretaceous shales in the WLB. Generally, illitization of the smectite becomes significant at 8,000 feet present-day depth and is largely complete by 9,500 feet present-day depth (**Figure 7**). This interval coincides with the transition between normally pressured, water-saturated Cretaceous shales above and anomalously pressured, hydrocarbon-saturated Cretaceous shales below in the WLB. The anomalously high percentage of illite present in the relatively shallow section of the Washakie Basin was caused by extensive basin inversion during the late Eocene (Roehler, 1992; **Figure 7**).

Organic geochemistry

Organic geochemical analyses performed on cuttings from the Mowry Shale in the WLB include vitrinite reflectance (R_0), anhydrous pyrolysis (reported as production index, (PI); Tissot and Welte, 1984), and solid-state ^{13}C nuclear magnetic resonance (reported as NMR spectra and carbon aromaticity).

R_0 is a measure of the thermal maturity of organic matter. The liquid oil generation window is generally thought to occur between R_0 values of 0.5 to 1.3 percent (Tissot and Welte, 1984). Oils thermally crack to wet gas at R_0 values of 1.3 to 2.0 percent. In the WLB, R_0 values increase slowly from 0.47 percent at 1,000 feet present-day depth to 0.6 percent at 9,000 feet, where the anomalously pressured Cretaceous shale section begins. R_0 values increase rapidly below this depth, from 0.6 percent at 9,000 feet to 1.7 percent at about 15,000 feet (**Figure 9**). Thus, the thermal maturation regime for Cretaceous shales above 9,000 feet depth (i.e., regional fluid flow boundary; lack of fluid flow across this regional boundary) probably differs from the thermal regime for shales below that depth.

Production indices (PI) are calculated as $S_1 /(S_1 + S_2)$, where S_1 is the amount of hydrocarbon present before pyrolysis and S_2 is the amount of hydrocarbon generated during pyrolysis. Like R_0, the PI values of the Cretaceous shales in the WLB increase slowly from 0.03 at 1,000 feet present-day depth to 0.1 at 9,000 feet present-day depth (**Figure 10**). Below these present-day depths, PI values increase rapidly from 0.1 at 9,000 feet to 0.4 at 14,000 feet (**Figure 10**). The PI values indicate that shales at greater than 8,000 to 9,000 feet present-day depth in WLB have experienced higher thermal exposure and therefore have undergone a different thermal history and a different thermal maturation regime than shales above this depth.

For a typical NMR spectrum, the x-axis scale (in ppm) is the chemical shift, a measure of the magnetic field strength required to cause a paramagnetic nucleus (^{13}C) to produce a resonance signal (Miknis et al., 1993). A paramagnetic nucleus that is shielded by electrons produces a signal that is shifted up-field (right) on the chemical-shift scale, and a paramagnetic nucleus that is de-sheilded by electrons produces a signal that is shifted downfield (left). In typical kerogen NMR spectra, the broad band between 0 and 60 ppm is associated with

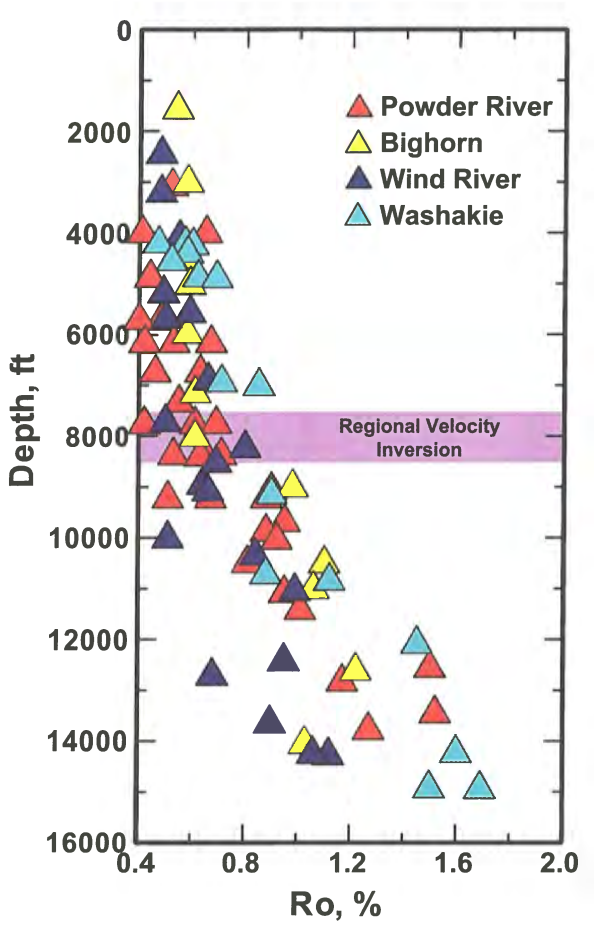

Figure 9. Plot of vitrinite reflectance (R_0) vs. present-day depth for the Cretaceous shales in the Wyoming Laramide basins. *Modified from Jiao and Surdam, 1997.*

aliphatic carbons with naphthenic structures. The broad band between 100 and 200 ppm is associated with aromatic and carbonyl carbon structures. Thus, NMR spectra can be used to study the abundance of ^{13}C nuclei in the various structural and functional groups in kerogen, and changes in kerogen structure associated with thermal maturation (Surdam and Crossey, 1985).

With progressive burial or thermal maturation, a decrease occurs in the peak area of the aliphatic functional group and an increase occurs in the peak area and sharpness of the aromatic functional group. This trend reflects changes in kerogen structure caused by thermal maturation (**Figure 11**). By 9,000 feet present-day depth, the aliphatic carbon peak is almost gone, and kerogen has virtually exhausted its capacity to generate liquid hydrocarbons and has little capacity to further generate gaseous hydrocarbons (**Figure 11**). This geochemical evidence

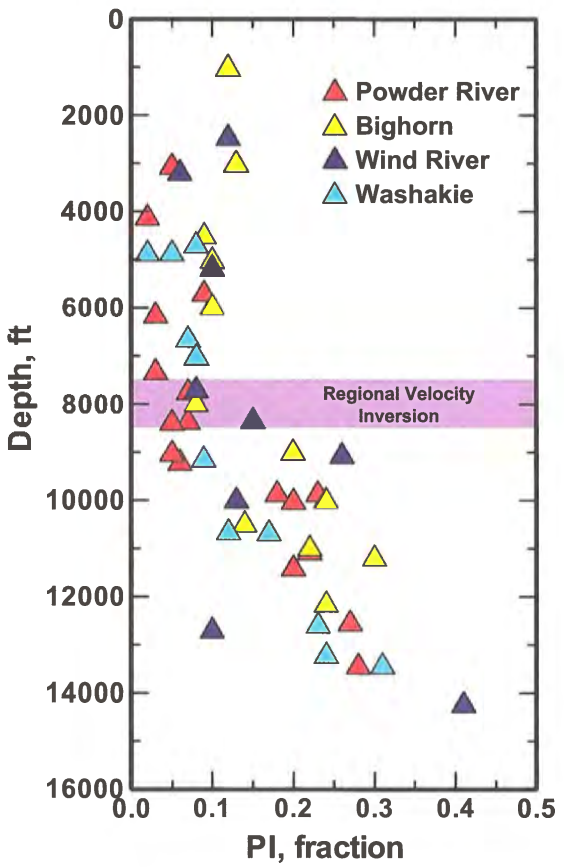

Figure 10. Plot of production index (PI) vs. present-day depth for the Cretaceous shales in the Wyoming Laramide basins. *Modified from Jiao and Surdam, 1997.*

indicates that the Mowry Shale in the WLB was at one time exposed to higher temperatures, which is consistent with both the R_0 and PI data.

The organic geochemistry values of the Mowry Shale are characterized by relatively low gradients to depths of 8,000 ± 1,000 feet present-day depth; below this depth, there is a rapid steepening of the pressure/depth gradient in the Cretaceous sandstones in the WLB (**Figure 12a** and **Figure 12b**; Surdam et al., 1995; Surdam et al., 1997). Thus, the geochemical changes and the onset of the anomalous pressure appear to be intrinsically linked.

Other maturation indicators such as T_{max} show similar depth trends. T_{max} values for the Mowry Shale samples increase from 410°C to 455°C with increasing depth (**Figure 13**). Again, like most of the maturation parameters for the Mowry Shale, the parameter/depth gradient shows a noteworthy steepening at the 8,000- to 9,000-foot present-day depth (i.e., at the regional fluid-flow boundary; normal hydrostatic pressures above and anomalous pressures, usually overpressure, below).

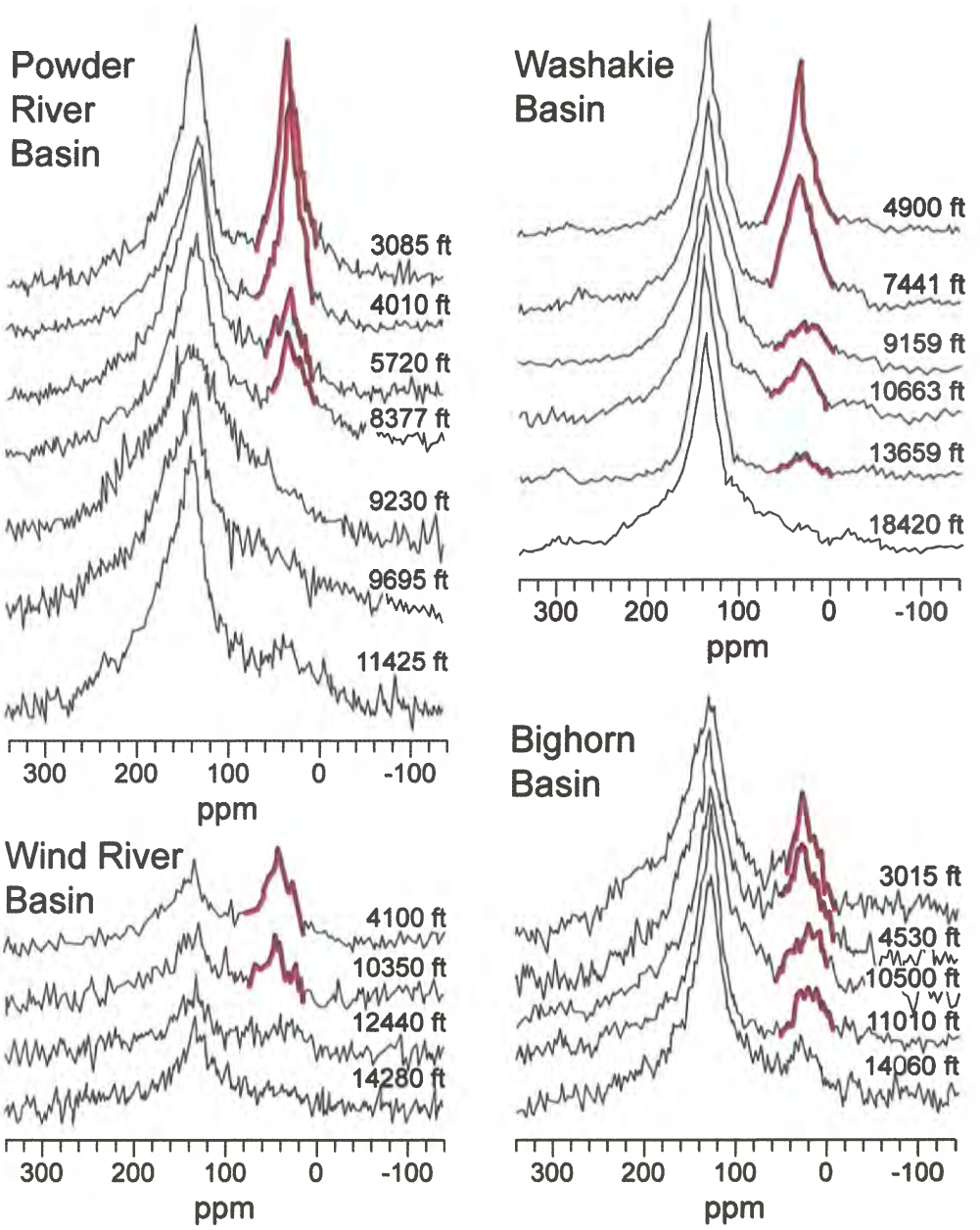

Figure 11. ^{13}C nuclear magnetic resonance (NMR) spetra of the Mowry Shale samples collected from depths of 3,000 feet to 18,000 feet in the Wyoming Laramide basins. Note that the aliphatic carbon peak (the right-hand major peak) diminishes or disappears at approximately 10,000 feet. *Modified from Jiao and Surdam, 1997.*

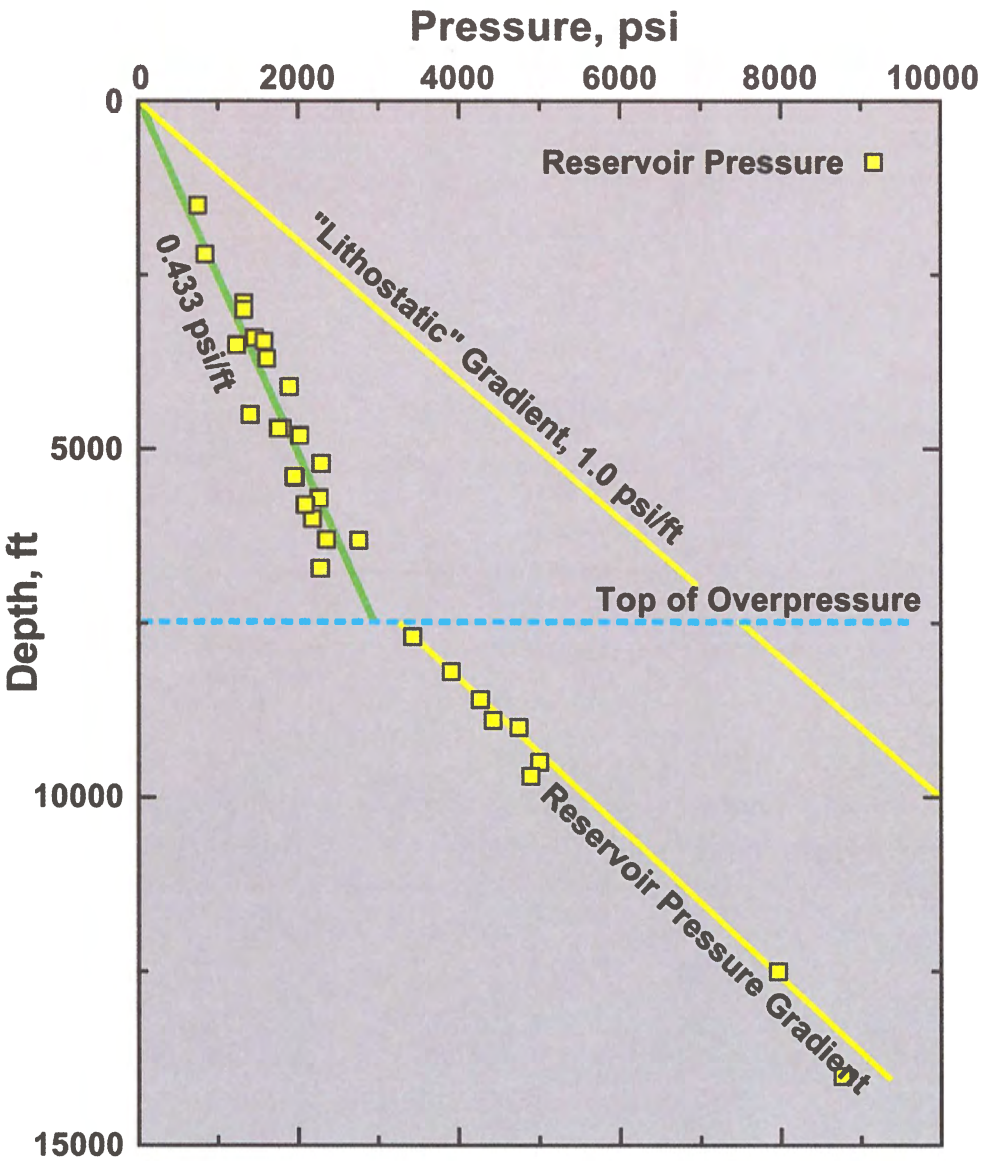

Figure 12a. Pressure profiles for the major Cretaceous gas reservoirs in the Washakie Basin. Note that at the depth at which compartmentalization is complete, the evolution of the pressure regime is significantly altered. Below the top of overpressure, the change of reservoir pressure parallels the lithostatic gradient, but is offset to lower pressures than the regional lithostatic gradient. *Modified from Surdam et al., 1997.*

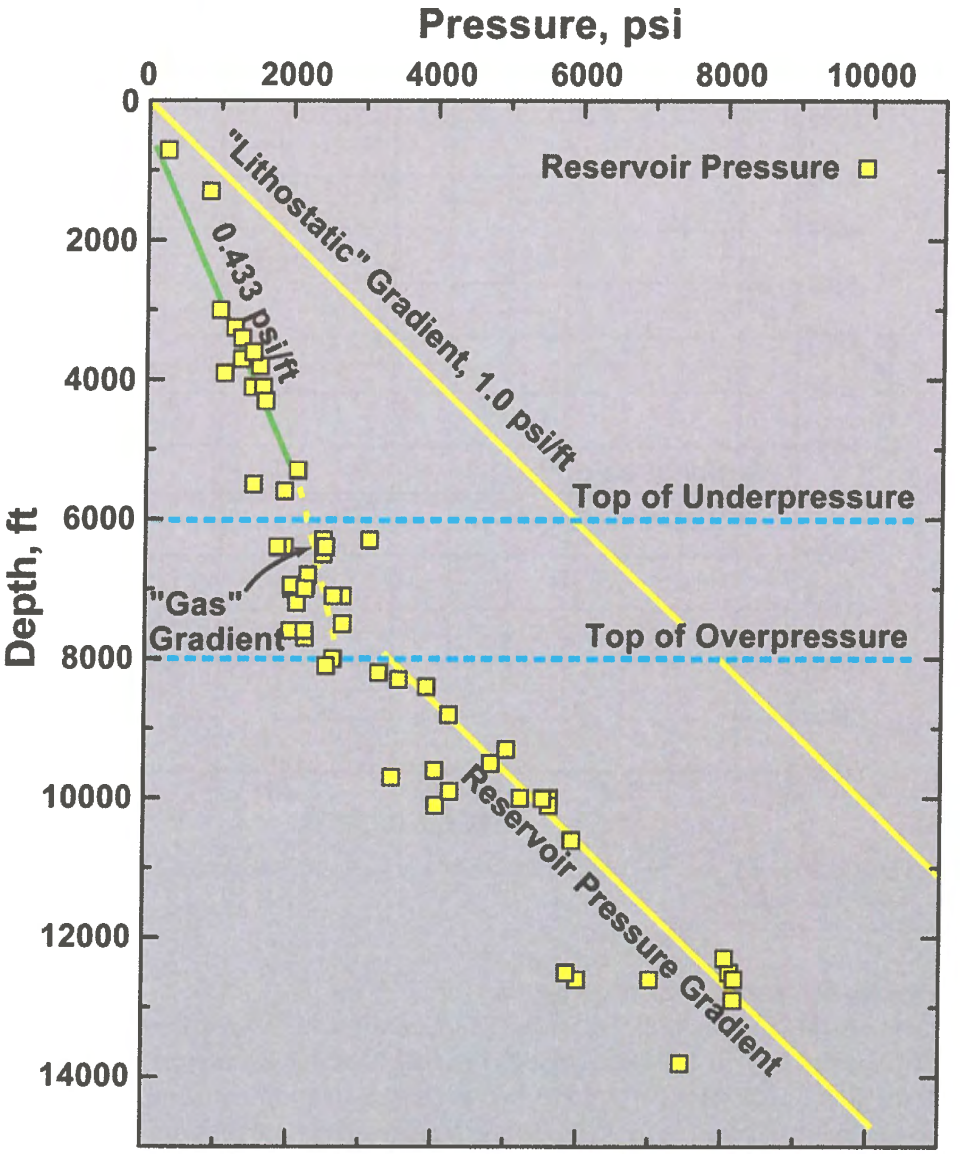

Figure 12b. Pressure profiles for the major Cretaceous gas reservoirs in the Powder River Basin. Note that at the depth at which compartmentalization is complete, the evolution of the pressure regime is significantly altered. Below the top of overpressure, the change of reservoir pressure parallels the lithostatic gradient, but is offset to lower pressures than the regional lithostatic gradient. *Modified from Surdam et al., 1997.*

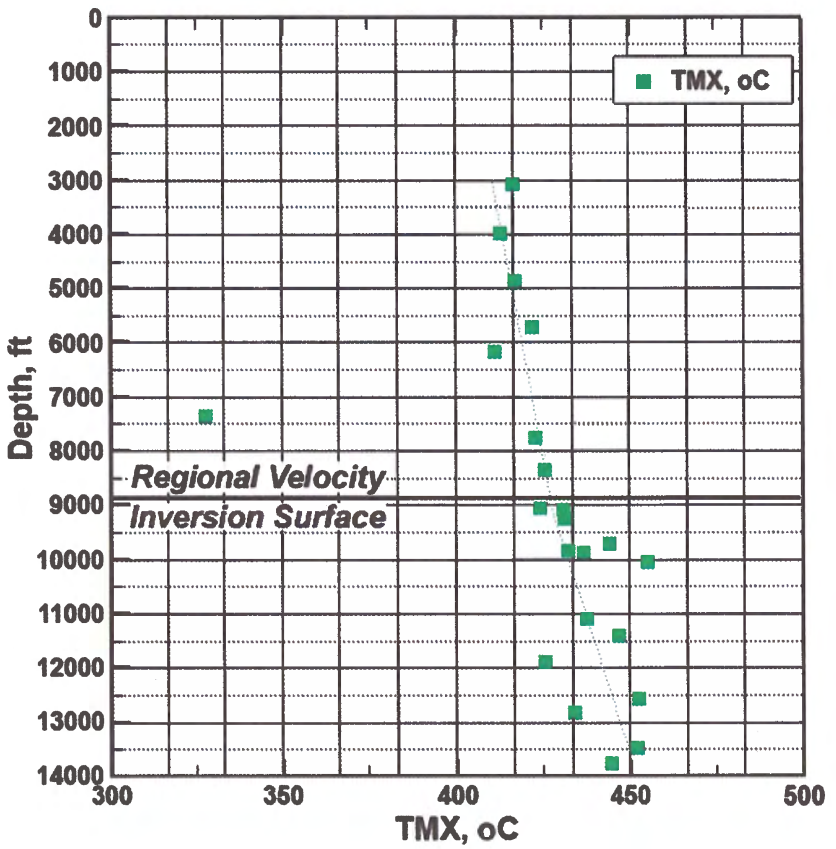

Figure 13. Plot of T_{max} vs. present-day depth for the Cretaceous shales in the Powder River Basin, Wyoming.

Sealing capacity and capillary seals

Most shales have highly ductile clay matrices, which cause them to have some of the lowest permeability values (10^{-7} to 10^{-4} millidarcies) of any of the various rock types under normal compaction (Best and Katsube, 1995). Because of their relative impermeability, shales are the most common seals present for hydrocarbon accumulations and pressure compartments (fluid-flow compartments); in fact, North (1985) indicates that shales act as seals for sandstone reservoirs in more than 60 percent of the known giant oil fields.

Certain petrophysical and flow properties of a rock unit determine the height of the hydrocarbon column that can be supported by a hydrocarbon/pressure seal, known as the *sealing capacity*: sealing capacity is a function of pore radius and fluid characteristics. In this study, we used Smith's (1966) equation to calculate the sealing capacity of Cretaceous shales:

$$H = \frac{(P_{dB} - P_{dR})}{0.433\ (\rho_w - \rho_h)}$$

where H is the maximum hydrocarbon column in feet that a seal can support, P_{dB} is the subsurface displacement pressure in psi of the seal rock, P_{dR} is the subsurface displacement in psi of the reservoir rock, ρ_w is the subsurface density in g/cm^3 of water, ρ_h is the subsurface density of the hydrocarbon, and 0.433 is a unit conversion factor.

In our investigation, 30 bulk shale samples from the Cretaceous section in the WLB were subjected to high-pressure mercury injection tests. The injection pressure curve (plateau portion) was extrapolated to 0 percent mercury saturation and, using Schowalter's (1979) nomograms, this pressure was converted to produce the displacement pressure (P_d) for each sample, for the subsurface gas/water and oil/water (multiphase) systems. Typical displacement pressure results for the Mowry Shale from the Powder River and Washakie basins are shown in **Table 1**.

For the gas/water system, the sealing capacity of the Mowry transgressive shales is a 600-foot gas column at a present-day depth of 5,500 feet, and rapidly increases to a 2,150-foot gas column at 8,000 foot depth and a 6,150-foot gas column at 13,000 foot depth. Displacement pressure also significantly increases with burial. At a present-day depth of 13,000 feet, transgressive shales can withstand a differential pressure of 4,000 psi (**Figure 14**).

Sneider et al. (1991) proposed a classification of hydrocarbon seal type based on sealing capacity. According to this classification, the sealing capacity of the Mowry Shale in the WLB increases dramatically below a present-day depth of about 8,000 feet. Note that the increase in sealing capacity coincides with progressive clay diagenesis as the structure of mixed-layer I/S clay changes from random to ordered at about 8,000 feet to 10,000 feet present-day depth (**Figure 7**); in other words, across the regional fluid flow boundary, the sealing capacity of the Cretaceous shales changes from B to A type according to the Sneider et al. (1991) classification (**Table 1**).

Calculations by Iverson et al. (1995) indicate that, based on single-phase fluid flow, even with an assumed permeability of only one nanodarcie (nd), a pressure differential will dissipate in one million years (m.y.) for a large reservoir, or 0.01 m.y. for a small reservoir. However, results from thermal maturation modeling indicate that overpressured compartments in the WLB have existed for at least 40 m.y. (Jiao, 1992; Surdam et al. 1995).

Investigation of the fluid-flow regimes of the Cretaceous shales in the WLB has helped account for the maintenance of this pressure differential through geologic time. For instance, the vertical trends of R_0, PI, clay diagenesis, and NMR spectra indicate that above 8,000 to 9,000 feet present-day depth, few hydrocarbons remain in the shales, and that below that

Table 1. Displacement pressure (P_d) and sealing capacity of the Cretaceous shales, Powder River and Washakie basins. *From Surdam and Jiao, 1997.*

Depth *(ft)*	Porosity ϕ *(%)*	Permeability K *(md)*	P_d (gas/water) *(psi)*	Sealing capacity (H) *(ft)* (gas column)
Powder River Basin				
5,500	11.7	0.012	400	600
7,900	5.2	0.059	1,300	2,000
8,000	5.6	0.013	1,500	2,300
8,800	2.9	0.012	1,800	2,700
9,900	2.7	N/A	2,800	4,300
10,000	2.2	0.004	3,000	4,600
13,000	2.2	0.004	4,000	6,100
Washakie Basin				
5,000	5.5	0.013	1,600	2,400
7,300	4.6	0.009	1,900	2,900
10,000	1.3	0.007	2,200	3,300
10,500	5.2	0.035	2,000	3,000
11,000	2.1	0.008	2,200	3,300
14,000	3.0	0.009	2,000	3,000

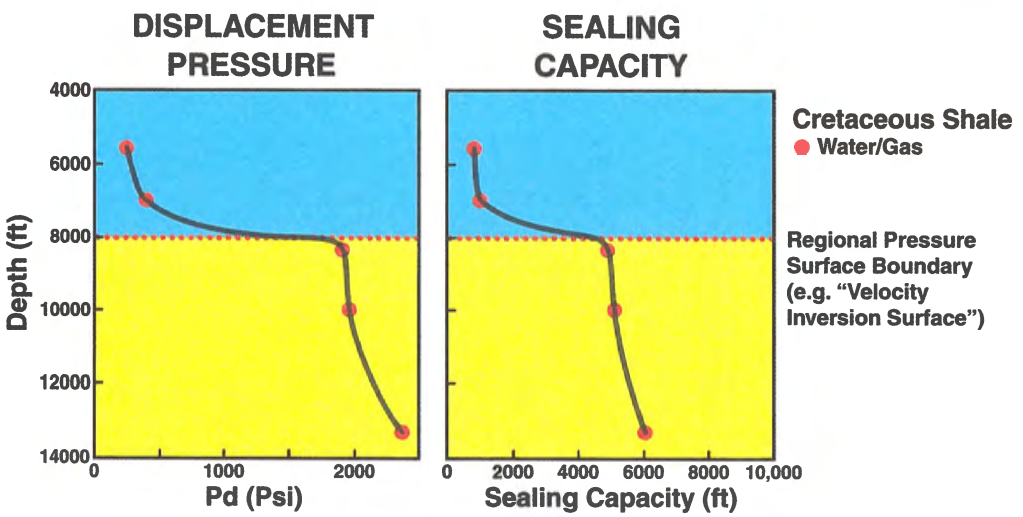

Figure 14. Plot of displacement pressure and sealing capacity vs. present-day depth for the Cretaceous shales in the Wyoming Laramide basins.

depth, significant quantities of hydrocarbons have been generated and retained by the shales. Above 8,000 to 9,000 feet present-day depth in the WLB, the Cretaceous shales are normally pressured and dominantly under water drive (i.e., a single-phase fluid-flow system). Below this depth, the shales are characterized by a multiphase fluid-flow system (oil/water or gas/oil/water), are dominantly under gas drive, and are typically overpressured (i.e., a multiphase fluid-flow system). With the addition of hydrocarbons to the system, these low-permeability Cretaceous shales become orders of magnitude more effective as overpressured media than they were in a single-phase (water) fluid-flow system. In fact, only in a multiphase system could displacement pressures measured in the laboratory be of the same order of magnitude as those observed in the Mowry system in the Powder River Basin of Wyoming. The relative permeability of the shales has more control over the system than their absolute permeability; in other words, the relative permeability is the effective permeability characterizing the fluid-flow system in the Cretaceous shales in these WLB. Thus, in a multiphase system, capillary pressure becomes very important in the formation of the pressure seals, compartment boundaries, and storage of hydrocarbons.

Burial history and thermal maturation

Four of the WLB were evaluated for burial history and thermal maturation of hydrocarbons: the Powder River, Wind River, Bighorn, and Washakie basins (**Figure 15**). We constructed isopach maps, structural contour maps, and maps showing the depth to the top of the Mowry Shale for the shale in each basin (**Figure 16a, b, and c**). From this information, coupled with data presented in the earlier portion of this paper, the burial and thermal maturation histories of the Mowry were interpreted for each of the four targeted basins (**Figure 17**). The typical thermal models for each of the WLB are very similar and can be summarized as follows: for Mowry Shale maximum burial to 10,000 feet or more, the thermal maturation models suggest that for each gram of TOC in the Mowry, about 80 milligrams (mg) of gas was generated, 18 mg of gas was expelled, and 62 mg of gas remains stored in the shale. Most importantly, approximately 75 percent of the gas generated within the Mowry Shale remains stored in the shale. This maturation scenario is credible because, as described, the Mowry Shale below a present-day depth of 8,000 feet in the WLB has displacement pressures of 2,000 to 3,000 psi (**Figure 14**); unless pressure builds up and exceeds these displacement pressures, or the shales are faulted and fractured, and connected to a fluid-flow system at lower pressures, the gas will not migrate out of the shale. The only escape mechanism for the gas in this capillary-dominated flow fluid system is to either 1) exceed the displacement pressure, or 2) exceed the fracture gradient through tectonic activity with resultant faulting, or fracturing of the rock. This same phenomenon explains why, in the WLB, the shale-rich Cretaceous stratigraphic section from approximately 8,000 feet present-day depth down to the lowermost Cretaceous organic-rich shales in the WLB is typically overpressured and gas-charged (Surdam et al., 2005).

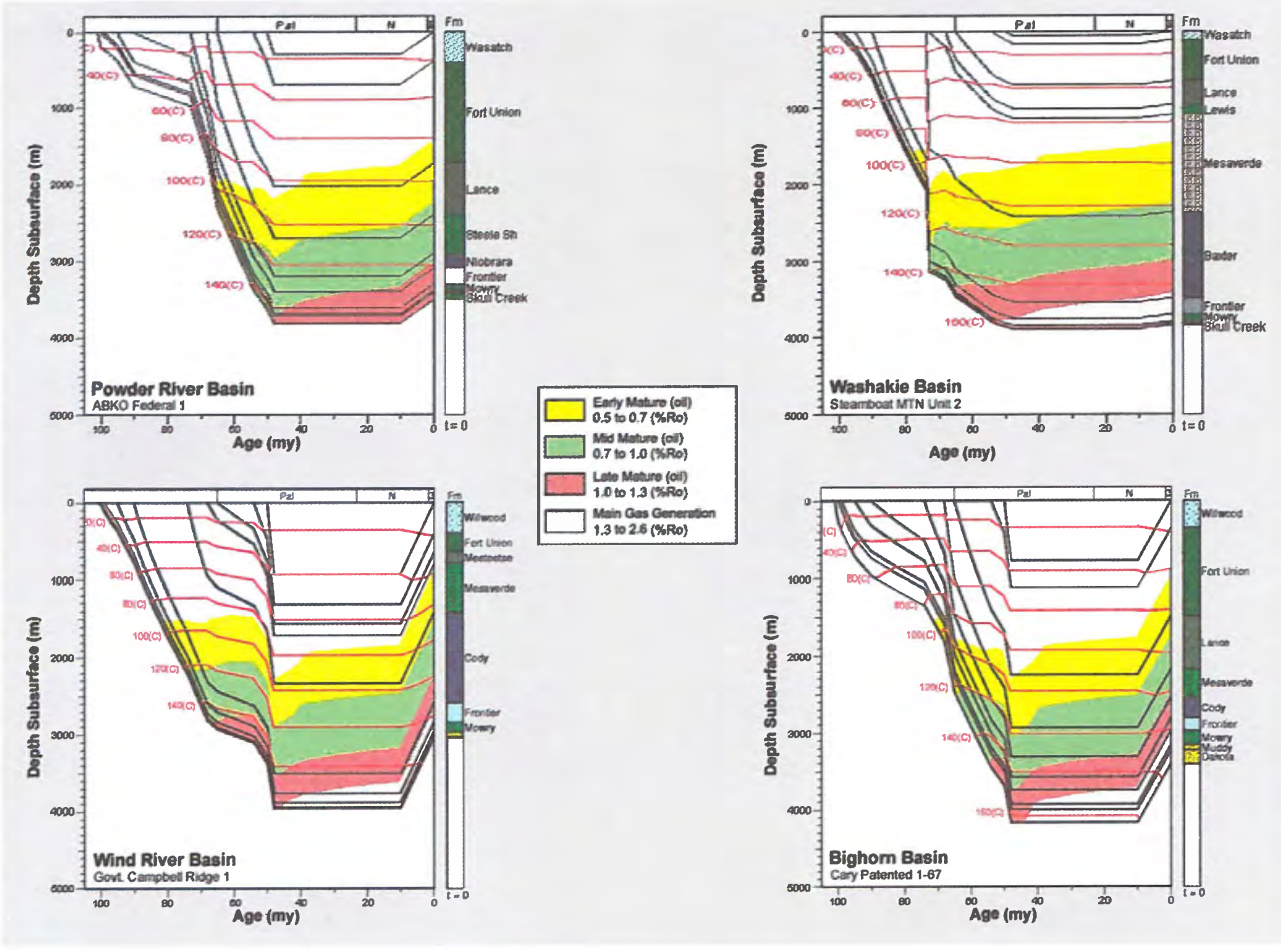

Figure 15. Reconstructions of burial and thermal maturation histories for the Powder River, Wind River, Bighorn, and Washakie basins, Wyoming. Isotherms are shown by red lines. The oil and gas generation stages are shown in yellow, green, and red.

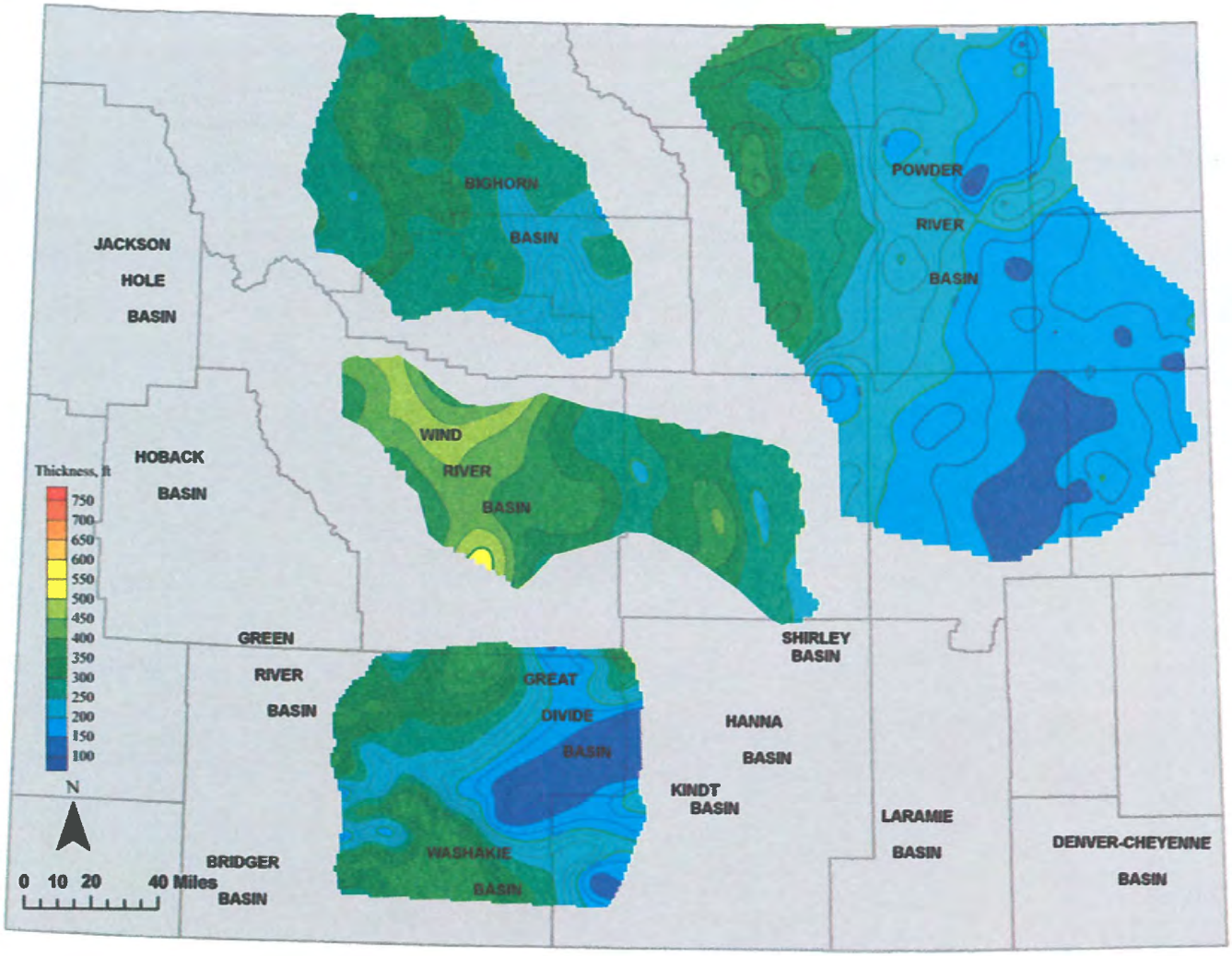

Figure 16a. Isopach maps of the Mowry Shale in the Powder River, Wind River, Bighorn, Washakie, and Great Divide basins, Wyoming.

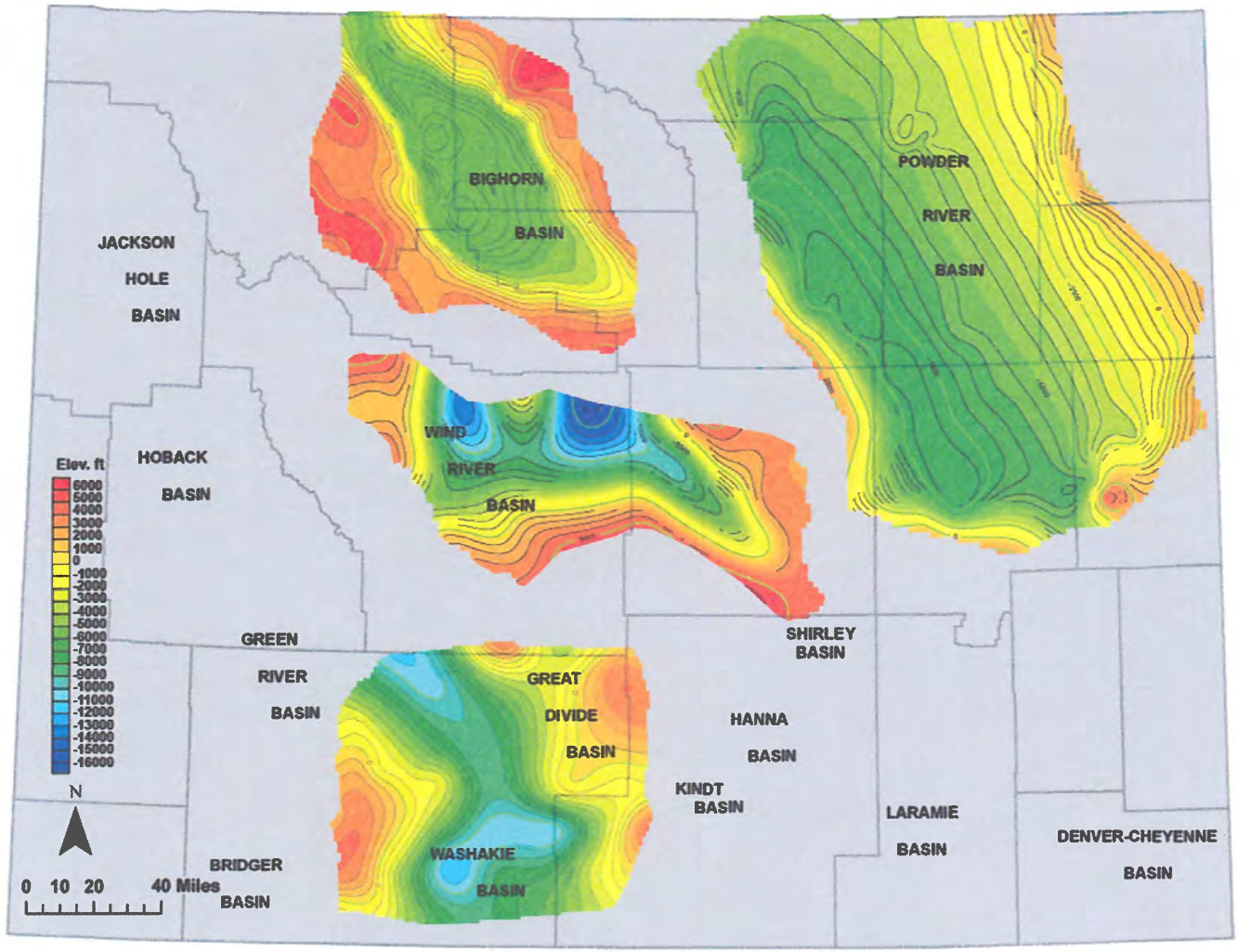

Figure 16b. Structural contour maps of the Mowry Shale in the Powder River, Wind River, Bighorn, Washakie, and Great Divide basins, Wyoming.

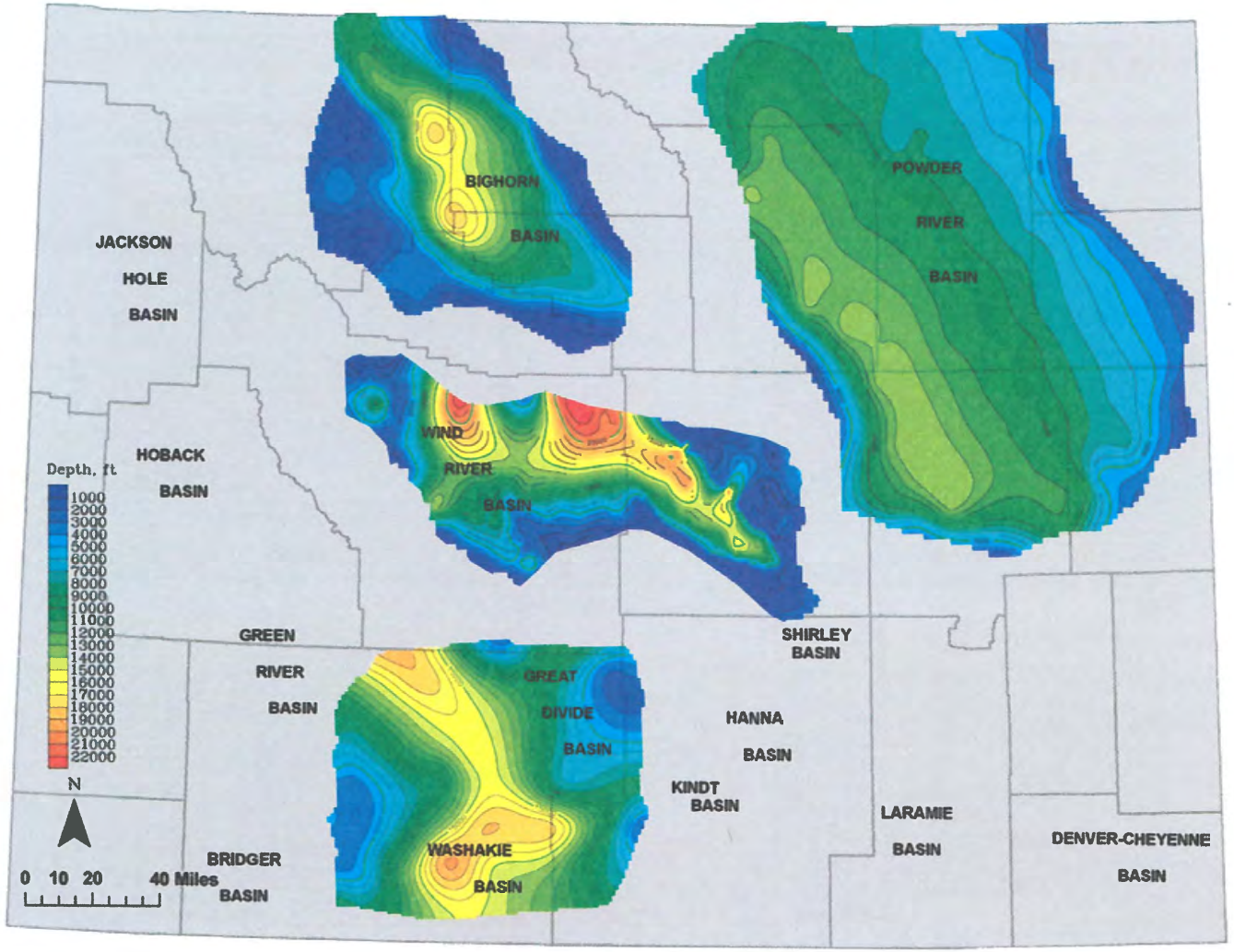

Figure 16c. Depth to the top of the Mowry Shale in the Powder River, Wind River, Bighorn, Washakie, and Great Divide basins, Wyoming.

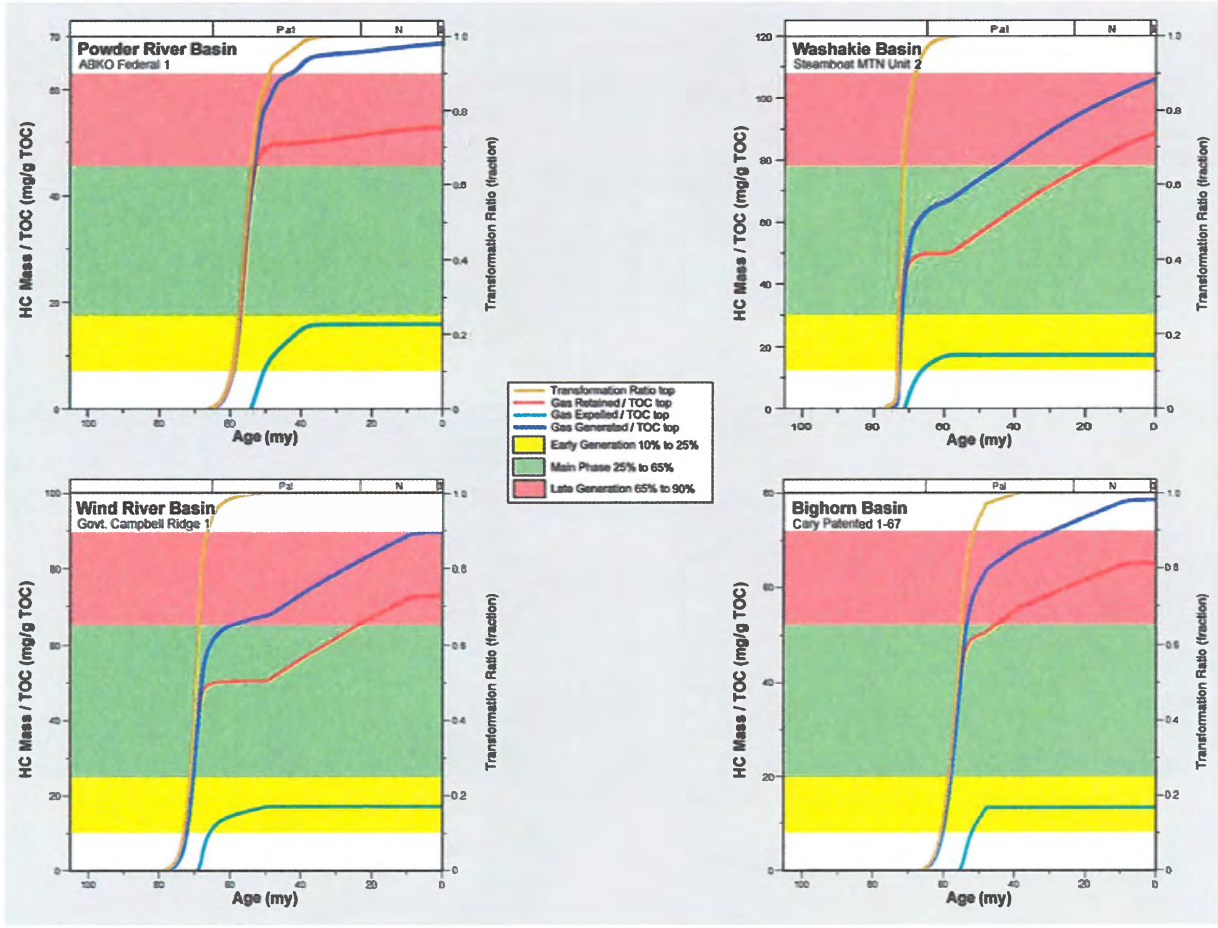

Figure 17. Plots of transformation ratio, gas generation, gas expulsion, and gas retention of the Mowry Shale in the Powder River, Wind River, Bighorn, Washakie, and Great Divide basins, Wyoming. Note that approximately 75 percent of the gas generated within the Mowry Shale remains in the shale.

Regional significance

The shale observations outlined above fit neatly with the regional fluid-flow systematics for WLB discussed by Surdam et al. (2005). In brief, in each WLB at 8,000 to 9,000 feet present-day depth in the dominantly low-permeability Cretaceous stratigraphic section, there is a regional seismic/sonic velocity slow-down associated with a transition from single-phase fluid-flow systems to multiphase fluid-flow systems. The multiphase portion of the fluid-flow system is dominated by capillarity and anomalous pressures, either over- or under-pressure (Surdam et al., 2005). This regional fluid-flow transition or boundary typically coincides with the presence of a low-permeability lithologic unit, but it may cut across stratigraphy within the shale unit. The compartmentalized regional fluid-flow system in the WLB generally extends down to the lowermost organic-rich Cretaceous shales in the basins. **Figure 18** provides a good example of the typical regional fluid-flow system characterizing each WLB.

In summary, in the central portion of each WLB is a regionally significant three-dimensional (3-D) domain – dominated by low-permeability lithologies and anomalous pressures – between approximately 8,000 feet present-day depth and the lowermost Cretaceous organic-rich shales. This 3-D anomalously pressured domain has a ubiquitous gas charge (Surdam et al., 2005).

Exploration implications

These Laramide regional basin-center gas-charged domains are prime areas for shale-gas plays. Critical in evaluating a potential WLB shale-gas play is the ability to detect and delineate storage sweet spots within the low-permeability unit of interest. In this context, the two most important characteristics of a potential storage sweet spot are relatively good porosity (i.e., enhanced porosity) and high gas saturation in the formation fluid. If the distribution of these two attributes can be determined for a shale-rich unit within the regional gas-charged domain, shale-gas plays can be successfully developed in the WLB.

Potential exploration strategies

One possible approach to delineating gas storage sweet spots in the regional gas-charged domain is the use of specific seismic attributes related to fluid composition. An example of this approach is the work at Jonah Field outlined in Surdam et al. (2001). In this work, the distribution of anomalously slow seismic velocities was used to detect and delineate gas storage sweet spots (see especially Figure 5 in Surdam et al., 2005). A problem with this type of approach is that more than one parameter may affect the velocity function. As previously noted, the velocity function can be affected by burial, erosional, tectonic, lithologic, and compaction effects, as well as the presence of a gas phase in the formation fluid (Surdam et al., 2005). However, if the velocity analysis is focused on a specific lithology, or on a shale unit characterized by a relatively constant lithology (such as the Mowry Shale) within the spatial context of the anomalously pressured domain, the uncertainty of the evaluation can be greatly reduced.

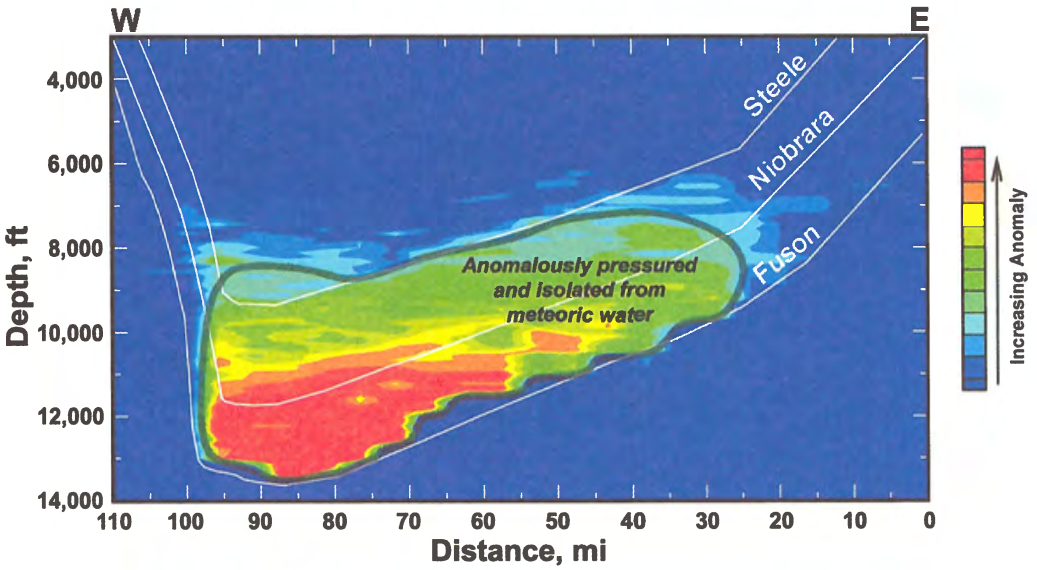

Figure 18. East-west anomalous velocity/fluid-flow system profile of the Powder River Basin, Wyoming. At 8,000 to 9,000 feet present-day depth in the dominantly low-permeability Cretaceous stratigraphic section, there is a regional seismic/sonic velocity slow-down associated with a transition from a single-phase fluid-flow system to a multiphase fluid-flow system, and from normal to anomalous pressures (Surdam et al., 2005).

For example, **Figure 19** shows the lateral velocity variation of the Mowry Shale on a two-dimensional (2-D) seismic line from the Bighorn Basin of Wyoming. Clearly, **Figure 19** shows significant lateral variations in seismic velocity within the Mowry Shale, a monolithic shale unit. It is suggested that these lateral velocity variations within the Mowry Shale over a distance of 0.5 miles are best explained by variations in the composition of the fluid phase (i.e., presence of gas). If the explorationist is convinced that substantial lateral variations in sonic/seismic velocity (up to 1,000 meters per second (m/s)) in relatively monolithic shale units are best attributable to variations in fluid composition, then a powerful tool exists to aid exploration for commercial shale-gas accumulations.

Consider the real case where the velocity attributes for the Mowry Shale were extracted from a 3-D seismic survey in the Greater Green River Basin. For the area of the survey, the approach outlined in Surdam et al. (2005) was used to develop an ideal velocity/depth gradient (i.e., baseline, or the velocity/depth gradient for the specific lithology assuming a single-phase fluid-flow system) for the Mowry Shale. Then, the "anomalous" velocity for the Mowry Shale below the regional velocity/pressure transition was determined by calculating the difference between the observed velocity for the Mowry Shale at a specific depth for the top, middle, or bottom of the shale unit, and the ideal velocity/depth gradient. The difference between the ideal and observed gradient is the anomalous velocity value for the Mowry Shale at that

specific depth. This procedure was used to laterally map the anomalous velocity function at the top of the Mowry over the area covered by the 3-D seismic survey (**Figure 20**). Figure 20 displays a clearly defined anomalously slow velocity area at the top of the Mowry Shale associated with an anticline. The velocity values for the Mowry Shale associated with the structure are 1,400 to 1,600 m/s slower than would be predicted by the ideal velocity/depth gradient; there is also a significant difference (approximately 1,000 m/s) between observed velocity values on the crest of the structure and values on the flanks of the structure. Again, we suggest that in this illustration (**Figure 20**), gas-filled enhanced porosity – probably due to fracturing – in the Mowry Shale on the anticline results in a detectable gas storage sweet spot (i.e., potential shale-gas play).

Vernik and Nur (1992) showed that the organic content of a shale can affect its velocity characteristics (**Figure 21**). So, velocity values of the Mowry Shale measured on and off of the structure shown in **Figure 20** were compared to the V_p/TOC curve for organic-rich shales measured by Vernik and Nur (1992). **Figure 21** shows that values for Mowry Shale samples collected on the structure are about 1,000 m/s slower than values for samples collected off the structure. This velocity difference in the Mowry Shale cannot be ascribed to variations in

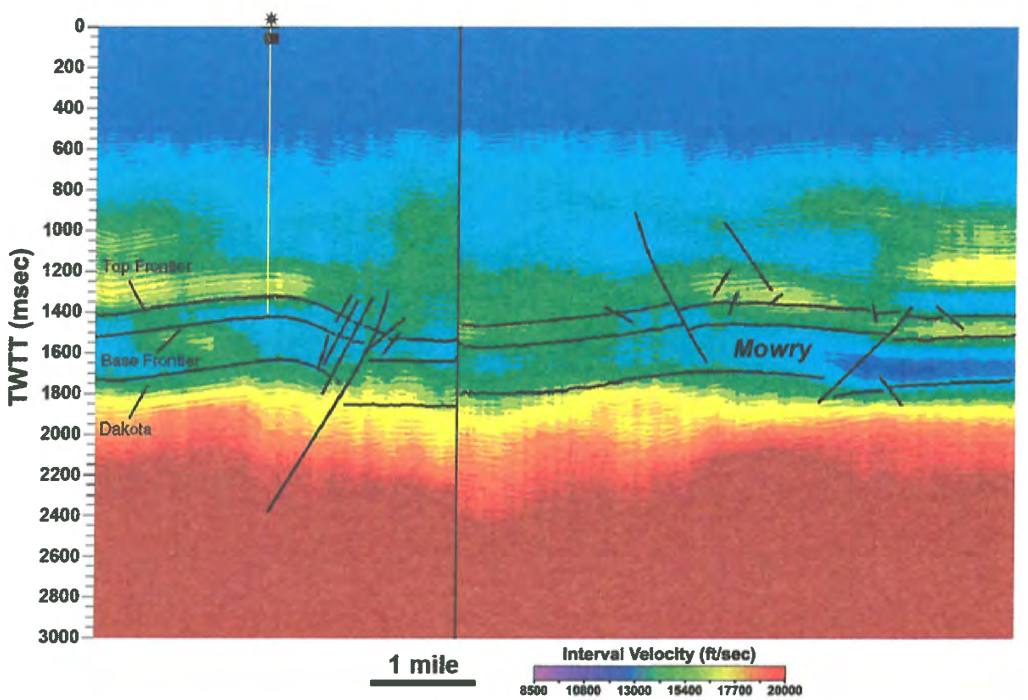

Figure 19. A seismic interval velocity profile from the Bighorn Basin. Note the significant lateral variation of interval velocity values within the Mowry Shale.

Figure 20. Anomalous velocity model of the Mowry Shale generated from a 3-D seismic survey in the Greater Green River Basin, Wyoming. A significant anomalously slow velocity domain, occurring at the top of the Mowry Shale and associated with an anticline, is clearly defined.

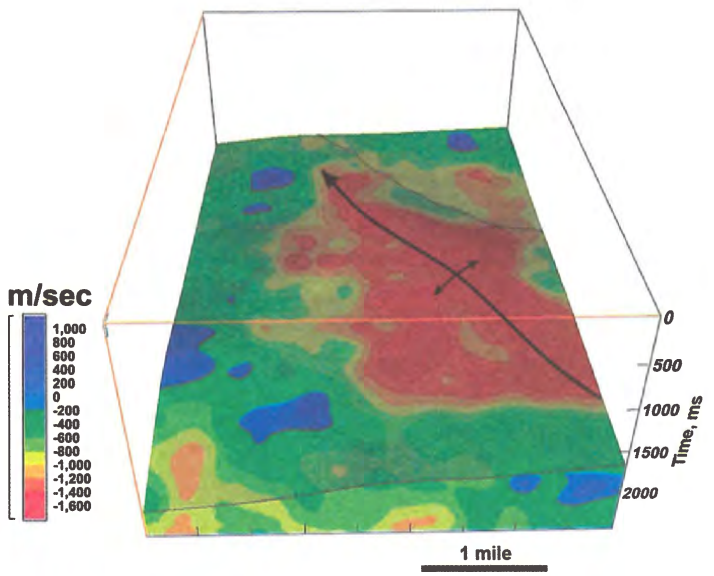

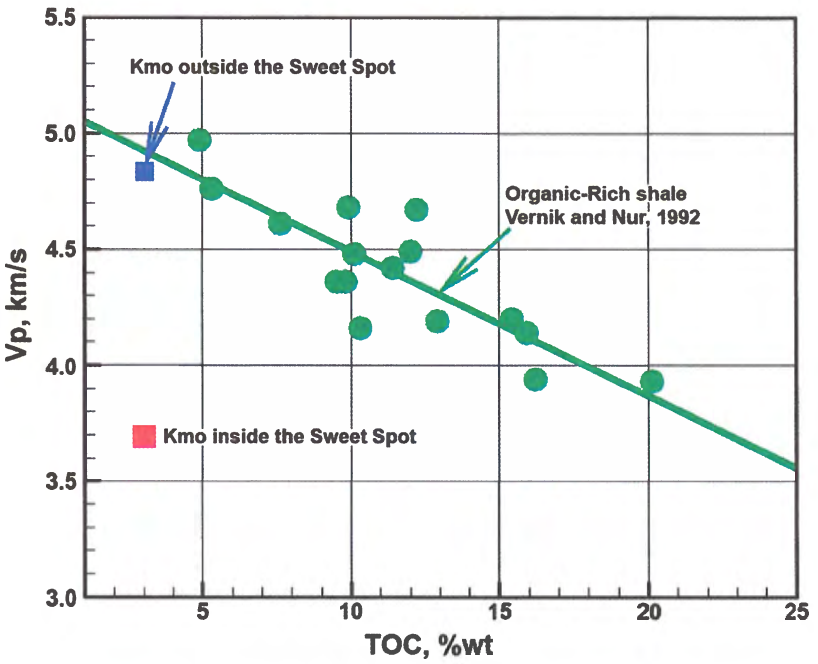

Figure 21. Plot of P-wave velocity vs. TOC showing how the organic content of a shale can affect its velocity characteristics. The velocities from Figure 20 on the structure (red square) and off the structure (blue square) from the 3-D survey used in Figure 20 are plotted on the figure, showing that there is significant lateral velocity variation within the Mowry Shale interval. *Modified from Vernik and Nur, 1992.*

organic content. Likewise, substantial velocity differences between shales separated laterally by 100 feet cannot be attributed to variations in lithology. Again, we suggest that the best explanation for the velocity distribution of the Mowry Shale shown in **Figure 20** is enhanced storage associated with the anticlinal structure and filled with gas.

Conclusions

The regional, Cretaceous, 3-D, gas-charged, anomalously-pressured domains (**Figure 18**) present in each of the WLB – from approximately 8,000 ± 1,000 feet present-day depth down to the lowermost Cretaceous organic-rich shales – are prime shale-gas targets. The basic characteristics of the Mowry Shale described in this work assist substantially in explaining the regional compartmentalization of fluid-flow systems and gas distribution inherent in the Cretaceous stratigraphic sections in the WLB. Moreover, seismic attributes can be used to accurately detect and delineate enhanced gas storage sweet spots within the regional gas-charged, anomalously pressured, low-permeability domains. If the Mowry Shale can be used as a surrogate for other organic-rich shales in the Cretaceous stratigraphic section, then most of the shale-rich stratigraphic units in the WLB have outstanding potential for shale-gas plays below the velocity inversion surface (**Figure 18**).

Acknowledgements

The authors would like to thank Wyoming Governor Dave Freudenthal and Rob Hurless, Energy and Telecommunications advisor to the governor, for their support. Allory Deiss and Meg Ewald provided outstanding graphical and editorial assistance. Discussions with Yuri Ganshin, a colleague at the WSGS, proved invaluable, as did contributions from other colleagues at the WSGS.

REFERENCES

Best, M.E., and Katsube, T.J., 1995, Shale permeability and its significance in hydrocarbon exploration: The Leading Edge, p. 165–170.

Boles, J.R., and Franks, S.G., 1979, Reply cementation of sandstones: Journal of Sedimentary Petrology, v. 49, p. 1362.

Bruce, C.H., 1984, Smectite dehydration and its relation to structural development and hydrocarbon accumulation in the Northern Gulf of Mexico Basin: Bulletin of the American Association of Petroleum Geologists, v. 68, p.673–683.

Burst, J.F., 1969, Diagenesis of Gulf Coast clayey sediments and its possible relation to petroleum migration: Bulletin of the American Association of Petroleum Geologists, v. 53, p. 73–93.

Byers, C.W., and Larson, D.W., 1979, Paleoenvironments of Mowry Shale (Lower Cretaceous), western and central Wyoming: Bulletin of the American Association of Petroleum Geologists, v. 63, p. 354–361.

Davis, J.C., 1970, Petrology of Cretaceous Mowry Shale of Wyoming: Bulletin of the American Association of Petroleum Geologists, v. 54, p. 487–502.

Davis, H.R., Byers, C.W., and Pratt, L.M., 1989, Depositional mechanisms and organic matter in the Mowry Shale (Cretaceous) of Wyoming: Bulletin of the American Association of Petroleum Geologists, v. 73, p. 1103-1116.

Dolsen, J.C., Muller, D.S., Evetts, M.J., and Stein, J.A., 1991, Regional paleotopographic trends and production, Muddy Sandstone (Lower Cretaceous), central and northern Rocky Mountains: Bulletin of the American Association of Petroleum Geologists, v. 75, p. 409–435.

Hagen, E.S., and Surdam, R.C., 1984, Maturation history and thermal evolution of Cretaceous source rocks of the Big Horn Basin, Wyoming and Montana, *in* Woodward, J., Meisser, F., and Clayton, J., editors, Hydrocarbon source rocks of the greater Rocky Mountain region: Rocky Mountain Association of Geologists, p. 321–338.

Hower, J., 1981, X-ray diffraction of mixed-layer clay minerals, *in* Longstaffe, F.J., editor, Clays and the resource geologist: Mineralogical Association of Canada, Short Course Handbook, v.7, p. 39–59.

Hower, J., Eslinger, E.V., Hower, M.E., and Perry, E.A., 1976, Mechanism of burial metamorphism of argillaceous sediments, 1, Mineralogical and chemical evidence: Geological Society of America Bulletin, v. 87, p. 725–737.

Iverson, W.P., Martinsen, R.S., and Surdam, R.C., 1994, Pressure seal permeability and two-phase flow, *in* Ortoleva, P., editor, Basin compartments and seals: American Association of Petroleum Geologists Memoir 61, p. 313–319.

Jiao, Z.S., 1992, Thermal maturation/diagenetic aspects of the abnormal pressure in Cretaceous shales and sandstones, Powder River Basin, Wyoming: Ph.D. dissertation, University of Wyoming, Laramie, 242 p.

Jiao, Z.S. and Surdam, R.C. 1997, Characteristics of anomalously pressured

Cretaceous shales in the Laramide basins of Wyoming, *in* R.C. Surdam, editor, Seals, Traps, and the Petroleum System: American Association of Petroleum Geologists Memoir 67, 243–254.

Kauffman, E.G., 1977, Geological and biological overview – western interior Cretaceous basin, *in* Kauffman, E.G., editor, Cretaceous facies, faunas, and paleoenvironments across the western interior basins: Mountain Geologist, v. 14, p. 75–99.

Miknis, F.P., Jiao, Z.S., MacGowan, D.B., and Surdam, R.C., 1993, Solid state NMR characterization of Mowry Formation shales: Organic Geochemistry, v. 20, p. 339–347.

North, F.K., 1985, Petroleum geology: Boston, Allen and Unwin, 607 p.

Obradovich, J.D., and Cobban, W.A., 1975, A time scale for the Late Cretaceous at the western interior of North America, *in* Caldwell, W., editor, The Cretaceous system in the western interior of North America: Geological Association of Canada Special Paper 13, p. 31–54.

Petty, E.A., Jr., and Hower, J., 1972, Late stage dehydration in deeply buried pelitic sediments: Bulletin of the American Association of Petroleum Geologists, v. 56, p. 2013–2021.

Pytte, A.M., and Reynolds, Jr., R.C., 1989, The thermal transformation of smectite to illite, *in* Naeser, N., and McCullock, T., editors, Thermal history of sedimentary basins: New York, Springer-Verlag, p. 133–140.

Roehler, H.W., 1992, Stratigraphy of the Upper Cretaceous Fox Hills Sandstone and adjacent parts of the Lewis Shale and Lance Formation, east flank of the Rock Springs Uplift, southwest Wyoming: USGS Professional Paper 1532, 57 p.

Schowalter, T.T., 1979, Mechanics of secondary hydrocarbon migration and entrapment: AAPG Bulletin, v. 63, no. 5, p. 723–760.

Smith, D.A., 1966, Theoretical considerations of sealing and non-sealing faults: Bulletin of the American Association of Petroleum Geologists, v. 50, p. 363–374.

Sneider, R.M., Stolper, K.K., and Sneider, J.S., 1991, Petrophysical properties of seals (abs.): AAPG Bulletin, v. 75, no. 3, p. 673–674.

Surdam, R.C., and Crossey, L., 1985, Mechanisms of organic-inorganic interactions in sandstone/shale sequences; relationship of organic matter and mineral diagenesis: SEPM Short Course Notes 17, p. 177–232.

Surdam, R.C., Jiao, Z.S., and Heasler, H.P., 1997, Anomalously pressured gas compartments in Cretaceous rocks of the Laramide basins of Wyoming: A new class of hydrocarbon accumulation, *in* Surdam, R.C., editor, Seals, traps, and the petroleum system: American Association of Petroleum Geologists Memoir 67, p. 199–222.

Surdam, R.C., Robinson, J., Jiao, Z.S., and Boyd, N.K. III, 2001, Exploration of the giant Jonah Gas Field using sonic and seismic data, Greater Green River Basin, Wyoming, *in* Anderson, D.S., Robinson, J.W., Estes-Jackson, J.E., and Coalson, E.B., editors, Gas in the Rockies: Rocky Mountain Association of Geologists Special Publication, Denver, p. 189–208.

Surdam R.C., Jiao, Z.S., and Ganshin, Y., 2005, A new approach to exploring for anomalously pressured gas accumulations: The key to unlocking huge, unconventional gas resources:

Wyoming State Geological Survey Exploration Memoir 1, 96 p.

Tissot, B.P., and Welte, D.H., 1984, Petroleum formation and occurrence 2nd ed.: Berlin, Springer-Verlag, 699 p.

Vernik L., and Nur, A., 1992, Ultrasonic velocity and anisotropy of hydrocarbon source rocks: Geophysics, v. 57, p. 727–735.

Williams, G.D., and Stelek, C.R., 1975, Speculations on the Cretaceous paleogeography of North America, *in* Caldwell, W.G.E., editor, The Cretaceous System in the Western Interior of North America: Geological Association of Canada Special Paper 13, p. 1–20.

ISBN 1-884589-55-3

WSGS-CS9-10